



PII:S0967-0661(97)00097-X

OPTIMAL THRUST ALLOCATION FOR MARINE VESSELS

O.J. Sørndalen*ABB Corporate Research, N-1361 Billingstad, Norway (ojs@nocrc.abb.no)**(Received December 1996; in final form May 1997)*

Abstract: This paper presents a new thrust-allocation scheme which significantly reduces the fuel consumption for dynamic positioning of ships when rotatable azimuth thrusters are used. Thrust allocation is the problem of determining the thrust and the direction of each of the n thruster devices of a ship, given the desired forces and moment from the control law. The problem of singular configurations is pointed out and solved by using a modification of the singular-value decomposition. A filtering scheme is proposed to control the azimuth directions to reduce the wear and tear, and to minimize the required thrust and power in a general manner, allowing the enabling and disabling of thrusters. Both new theory and full-scale sea trials are presented.

Copyright © 1997 Elsevier Science Ltd

Keywords: Ship control, thrust allocation, singularities, filtering

1. INTRODUCTION

The control of ships and marine vehicles has been studied for decades. Advanced control theory using optimal control and Kalman filtering was successfully used in (Balchen *et al.* 1980) for the dynamic positioning of ships. See (Fossen 1994, Sørensen *et al.* 1996) for further references. Ship control has mainly been focused on filtering techniques to avoid the influence from high-frequency wave-induced disturbances on the rudders and thrusters. Moreover, adaptation and estimation have been used to determine the desired forces in the surge and sway directions, and the moment in the yaw direction, to be generated by the propulsion system. Less focus has been put on the thrust-allocation problem, i.e. how much thrust should be provided by each of the n thruster devices, given the desired resulting forces and moment from the higher-level controller. In the case of rotatable azimuth thrusters, the orientation of the azimuths has to be determined, too. The classical way of solving the thrust-allocation problem is to solve a static quadratic minimization problem with constraints at each sample,

(Jensen 1980, Lindfors 1993). The basic assumption has been that azimuth thrusters can be considered as two independent perpendicular fixed thrusters without constraints on the rotational velocity.

This paper shows that, in general, one cannot consider an azimuth thruster as two independent fixed thrusters, due to mechanical constraints and to the operational constraint of slowly varying azimuths to minimize wear and tear. It is further shown that constraints on the azimuth rotations can lead to singular configurations. In these configurations, infinite thrust has to be provided by the propulsion system to satisfy the desired resulting surge and sway forces and yaw moment given by the control law. The problem of singular configurations does not occur if there is a sufficient number of enabled thrusters with fixed direction. However, a general thrust-allocation algorithm should be able to handle a situation with different types of thruster, propeller, and rudder configurations, and with various numbers of devices enabled for active control. In this paper, all thrust devices, such as propellers, azimuths, and tunnel thrusters, are denoted "thrusters" for

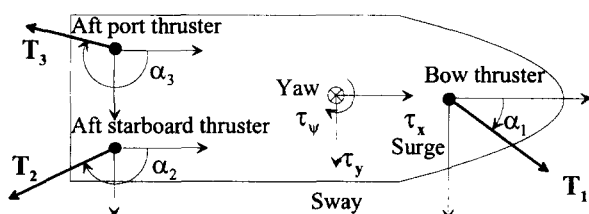


Fig. 1. Illustration of azimuth thrusters and notation.

simplicity. The important problem of singular configurations and explosion where infinite thrust is required has not previously been noted in the ship control literature. In addition to pointing out the singularity problem, it is shown in this paper how the problem of required infinite thrust close to singular configurations can be solved. Moreover, a scheme is proposed to control the azimuth directions to minimize the thrust and power needed. Simulation results from the dynamic positioning of a ship with three azimuth thrusters are shown, where models of environmental disturbances such as wind, waves, and current are included. Aspects of the theory on thrust allocation was presented in (Sørvalen 1996). Here, experimental results from full-scale sea trials are presented, showing a significant fuel reduction with the proposed thrust allocation.

2. PROBLEM STATEMENT

The thrust allocation determines the azimuth directions and the thrust for each thruster, given the desired forces in surge and sway, and the moment in the yaw direction from the controller. The forces in surge and sway and the moment in the yaw direction are denoted by the vector $\tau = [\tau_x, \tau_y, \tau_\psi]^T$, and the thrust from the n thruster devices is denoted by the vector $T = [T_1, T_2, \dots, T_n]^T$, as illustrated for a typical ship in Fig. 1. It is assumed that the thrusters are bi-directional, i.e. the thrust T_i can be negative. The commanded forces and the moment from the controller are denoted by $\tau_c = [\tau_{xc}, \tau_{yc}, \tau_{\psi c}]^T$. The directions of the thrusters are denoted by $\alpha = [\alpha_1, \alpha_2, \dots, \alpha_n]^T$.

The commanded forces and moment vector τ_c is derived from a control law that usually involves estimation and wave filtering, as in (Sørensen et al. 1996). In the dynamic positioning of ships one is concerned about keeping the low-frequency part of the position and/or heading at the reference. One is not interested in compensating for high-frequency disturbances such as wave induced motions, since this compensation would increase the fuel consumption without increasing the performance, and would increase the wear and tear on the propulsion equipment.

Active use of the azimuths can reduce the fuel consumption, and is necessary in the case of low thrust capacity. Minimal fuel consumption is obtained with fast-varying azimuth thrusters since the azimuths can then be oriented in the direction where the fuel consumption is minimal at each time instant. However, there is a trade-off between the minimal fuel consumption that is obtained with fast-varying azimuth direction control, and the minimal wear and tear which is obtained with slowly varying azimuth direction control. The requirement of slowly varying azimuths, together with the fact that the angular velocity of the azimuths is limited by a mechanical time constant imply that an azimuth thruster cannot be considered to have two degrees of freedom to the same extent as two independent, perpendicular, fixed thruster devices.

The reduction in the degrees of freedom can lead to singular configurations when the azimuths are used actively. In a singular configuration there are vectors τ_c (commanded surge and sway forces, and yaw moment) that cannot be obtained by applying finite thrusts T from the thruster devices. The singular configurations can be analyzed mathematically. Denote by $\alpha = [\alpha_1, \dots, \alpha_n]^T$ the vector of azimuth directions. Then, there is a relation between the vector T of thrusts from the thruster devices and τ , the resulting forces and moment acting on the ship from the propulsion system, given by

$$A(\alpha)T = \tau \quad (1)$$

where A is a matrix that depends on the thruster locations and is a function of the azimuth angles α . Here, normalized A and τ are considered. The singular values of A can be considered as gains from the thrust T to forces and moment τ in certain directions. The smallest singular value of A describes the ability to obtain all combinations of forces and moment τ . A singular value equal to zero implies that there are combinations of surge and sway forces and yaw moments τ that are impossible to obtain. The smallest singular value is plotted in Fig. 2 for the ship from Fig. 1, where there are three azimuth thrusters. In Fig. 2 the bow azimuth thruster is heading toward starboard, i.e. $\alpha_1 = 90^\circ$.

To illustrate that the smallest singular value can be small also for other configurations for the bow thruster, the area where the smallest singular value of $A(\alpha)$ is less than 0.015 is plotted in Fig. 3 for the case where the direction of the bow azimuth is 0° . It is seen that also in this case where the bow thruster is heading in surge direction, there are many combinations of directions for the two aft thrusters leading to small singular values

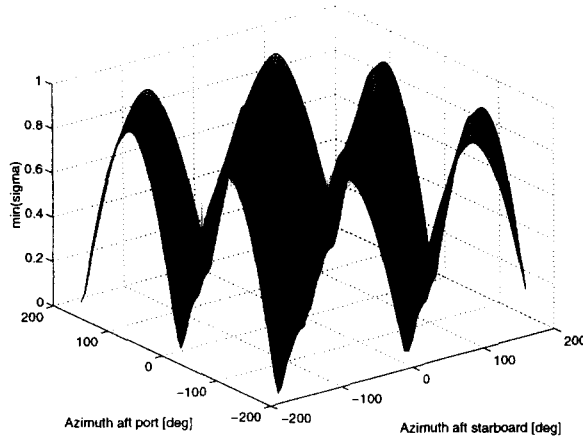


Fig. 2. Smallest singular value of $A(\alpha)$ as function of α_2 and α_3 with $\alpha_1 = 90^\circ$.

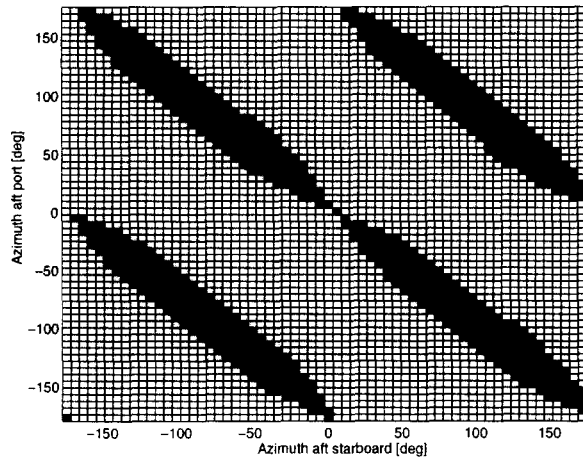


Fig. 3. Area of α_2 and α_3 where the smallest singular value of $A(\alpha)$ is less than 0.015 with $\alpha_1 = 0^\circ$.

and hence high gain from commanded forces and moment to required thrust.

A physical interpretation of these figures is that when the directions of the azimuths are e.g. all 90° (Fig. 2) the smallest singular value is zero since the azimuths cannot provide any force components in the surge direction. Hence, the azimuths are in a singular configuration. On the one hand the (many) singular configurations are undesirable because of the possible demand for great thrust. On the other hand, the required thrust is minimal in the singular configurations if no force components are commanded in the uncontrollable directions; e.g. if only the sway forces and yaw moment are non-zero in the case above.

One solution to avoid the needs for great thrust due to singular configurations might be to impose constraints on the azimuth angles. For the ship in Fig. 1, one engineering solution might be to prevent the two aft azimuths from being parallel by imposing e.g. the constraint $\alpha_3 = \alpha_2 + \frac{\pi}{6}$ on the system. This solution would eliminate the singular configuration $\alpha = [\frac{\pi}{2}, \frac{\pi}{2}, \frac{\pi}{2}]^T$. However, there are

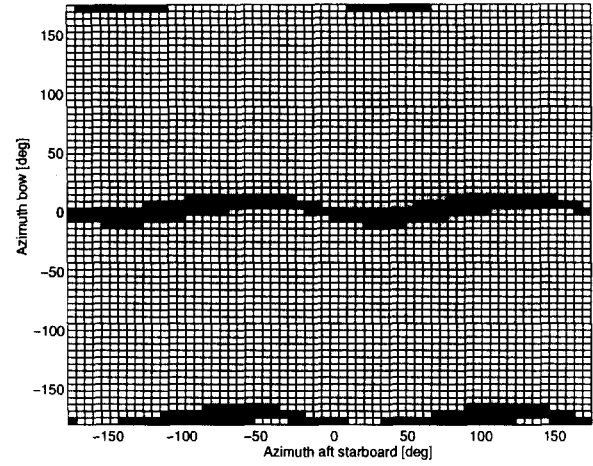


Fig. 4. Area of α_1 and α_2 where the smallest singular value of $A(\alpha)$ is less than 0.05 with $\alpha_3 = \alpha_2 + \frac{\pi}{6}$.

still infinitely many singular configurations, as shown in Fig. 4, where the smallest singular value is plotted as a function of α_1 and α_2 .

Hence, the singularities are difficult to avoid. For a ship with three enabled thrusters like the ship in Fig. 1, it is easy to show that for all $i \in \{1, 2, 3\}$

$$\det A(\alpha_i) = -\det A(\alpha_i + \pi)$$

where the variable α_i is the i -th azimuth angle. The determinant function is a continuous function of the azimuth angles. Since $\det A(\alpha)$ changes sign when an azimuth thruster rotates by 180° , the thruster configuration has to pass through a singularity α_s where $\det A(\alpha_s) = 0$, which is equivalent to the smallest singular value of $A(\alpha_s)$ being zero.

The control problem is: given τ_c , determine the thrusts T and the orientations of the active azimuths α so that

- (1) $\|A(\alpha)T - \tau_c\|$ is small, to minimize the control error
- (2) $\|T\|$ is small, to minimize the fuel consumption
- (3) $\alpha_i(t)$ is slowly varying, to minimize wear and tear on the azimuth thruster devices.

In addition, the problem is also to find a general solution satisfying the above constraints for fewer thrusters than the dimension of the command vector τ_c , to enable control also in the case of thruster failures or the manual disabling of some of the thrusters. Traditionally, thrust allocation has been studied for a constant number of thruster devices, higher than the dimension of command vector.

The solution approach presented here can be outlined as follows:

- First, the azimuth angles α are chosen to be the directions that minimize the thrust and counteract the **mean** environmental force over a given time period. These directions are found by using a filtering technique, with particular attention paid to 180° turns in the cases of non-symmetrical azimuth thrusters.
- Then, given the azimuth angles, the thrusts T are chosen to satisfy items (1) and (2) above. However, these constraints can be contradictory. A trade-off is found by considering the singular values of $A(\alpha)$.

3. FILTERING AND CONTROL OF AZIMUTH ANGLES

In this section, the azimuth angles α are determined, based on the commanded thrust and moment τ_c . The matrix $A(\alpha)$ from eq. (1) relates the thrusts T from the thruster devices to the resulting force and moment τ . Note that τ denotes the resulting forces and moment, as opposed to τ_c which denotes the commanded ones. The thrusts provided by the rotatable azimuth thruster devices can be decomposed into two components: one in the surge direction and one in the sway direction. Denote by T_e the extended thrust vector which includes all the azimuth components. The vector T_e is of length $n+m$, where n is the number of thruster devices, and $m \leq n$ is the number of rotatable azimuth thrusters. Denote by A_e the corresponding extended matrix which relates T_e to τ :

$$A_e T_e = \tau.$$

Now, define T_{ed} by $T_{ed} \triangleq A_e^+ \tau_c$ where A_e^+ is the pseudo-inverse of A_e , implying that if $\text{rank } A_e \geq \text{length}(\tau_c)$, then T_{ed} satisfies $A_e T_{ed} = \tau_c$ and $\|T_{ed}\|_2$ is minimal. If $\text{rank } A_e < \text{length}(\tau_c)$, then T_{ed} minimizes $\|A_e T_e - \tau\|_2$. Hence, the vector T_{ed} consists of the optimal surge and sway components of the azimuths, given τ_c . From these components it is straightforward to derive the azimuth angles α by calculating arctan of the relations of the sway and surge components of T . However, since the azimuth angles α are required to be slowly varying, the angles derived from T_{ed} cannot be applied directly since τ (and hence T_{ed}) are not constrained to be slowly varying. Therefore, a low-pass filtered version of T_{ed} will be used to derive the slowly varying azimuth angles. The mathematical expressions for the thrust direction filtering is quite involved. Hence, only the structure is described here.

The structure for deriving the low-frequency, desired azimuth angle α_f of a given thruster is shown in Fig. 5, where T_d denotes the two-dimensional vector force from T_{ed} corresponding to the actual

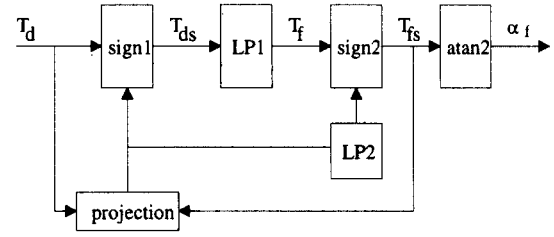


Fig. 5. Structure for deriving slowly varying azimuth angles.

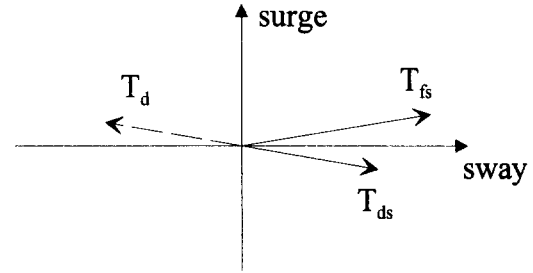


Fig. 6. Illustration of the need for turning T_d .

azimuth thruster. The direction of this vector T_d is changed by 180° , or equivalently the two components change sign, depending on the sign of the projection of T_d on the vector T_{fs} . The reason for this change is explained below by referring to Fig. 6. The resulting vector T_{ds} goes through a low-pass filter with a given bandwidth to form the slowly varying force vector T_f . If the direction of T_d has been more frequently changed than unchanged in sign1 over a given time interval, specified in the low-pass filter LP2, then the direction of T_f is changed by 180° in sign2. The reason for changing the direction of T_f , and thereby turning the azimuth thruster through 180° , is that the azimuths are usually more efficient when applying positive thrust than negative. Hence, if the azimuth thruster has applied more negative thrust than positive thrust over a given time interval specified in LP2, it then becomes more efficient to turn the azimuth thruster to the opposite direction. The sign2 function can be substituted by a hysteresis function to avoid possible frequent 180° turns. The reason for the sign1 function is illustrated in Fig. 6. If the projection of the vector T_d on T_{fs} has the opposite direction to T_{fs} , then T_{ds} , the opposite vector of T_d , should be used to update the slowly varying vector T_f , and thereby T_{fs} . In Fig. 6, the vector T_{fs} should be adjusted clockwise and not counter-clockwise to determine the azimuth angle α , since negative thrust can be applied.

Given the vector of filtered thrust components T_{fs} , one gets the (slowly varying) azimuth angle α_f from

$$\alpha_f = \text{atan2}(T_{fs}^y, T_{fs}^x) \quad (2)$$

where T_{fs}^x and T_{fs}^y represent the surge and sway force components of the actual azimuth thruster.

With the filtering proposed here, the mean values of the desired azimuth angles are obtained. Also, frequent turns of 180° of the azimuths due to e.g. wave disturbances are prevented, as opposed to schemes where the azimuths are considered as two independent thruster devices.

4. CONTROL OF THRUST AND SINGULARITY HANDLING

Given the orientations α_f of the thruster devices that were derived in the previous section, the thrusts from each of the thruster devices have to be determined. It is assumed that the thrusters are bi-directional, i.e. the components of T can be negative. As discussed in Section 2, a simple pseudo-inversion of (1) resulting in

$$T = A^+(\alpha_f)\tau_c \quad (3)$$

where A^+ is the pseudo inverse of A would lead to relatively large $\|T\|$ when α_f is close to singular configurations. Since singularities can occur with the active use of azimuths, a more advanced thrust controller has to be applied.

Assuming that the filtered azimuth angles represent the optimal thruster configuration for the mean τ_c , which reflects the mean environmental disturbances, then the singular values represent an ordering of the importance of the corresponding directions to satisfy equation (1) with minimal thrust T . Therefore, the small singular values that cause high thrust close to singularities represent directions off the mean direction of the environmental disturbances. The approach proposed here to determine T avoids the problem of high thrust, and provides effective "geometrical" filtering of the high-frequency disturbances.

The **singular value decomposition** states that any $m \times n$ matrix A can be factored into (Strang 1980),

$$A = USV^T$$

where U is an $m \times m$ orthogonal matrix, V is an $n \times n$ orthogonal matrix, and S is $m \times n$, having the following structure

$$S \triangleq \begin{bmatrix} \sigma_1 & & & \\ & \ddots & & \\ & & \sigma_r & \\ & & & \end{bmatrix}$$

where σ_i are the singular values of A and r is the rank of A . The singular values are positive and ordered so that $\sigma_i \geq \sigma_{i+1} > 0$. The pseudo

inverse of A is given by $A^+ = VS^+U^T$ (Strang 1980) where

$$S_{ii}^+ = \frac{1}{\sigma_i}. \quad (4)$$

Here, let A be $A(\alpha_f)$, $m = \text{length}(\tau_c) = 3$, and n be the number of (enabled) thruster devices. Hence, a solution of the equation $A(\alpha_f)T = \tau_c$ is $T = VS^+U^T\tau_c$ or

$$\tilde{T} = S^+\tilde{\tau}_c \quad (5)$$

where $\tilde{T} = V^T T$ and $\tilde{\tau}_c = U^T \tau_c$. Since U and V are orthogonal, the vectors \tilde{T} and $\tilde{\tau}_c$ can be considered as pure rotations of the vectors T and τ_c , respectively.

From (4,5) it is seen how the singular values can be considered as gains from T to τ . From (4) it is also seen that singular values close to zero result in relatively large $\|\tilde{T}\|$, or equivalently $\|T\|$, in the case of corresponding non-zero components in $\tilde{\tau}_c = U^T \tau_c$ if the solution (3), or equivalently (5), is applied.

The approach proposed here to determine the thrust T is given by

$$T = VS_\delta^+U^T\tau_c \quad (6)$$

where

$$S_{\delta,ii}^+ = s_i$$

where $i \in \{1, 2, \dots, r\}$ and for parameters $\delta_{hi} \geq \delta_{lo} > 0$

$$s_i = \begin{cases} \frac{1}{\sigma_i} & \text{if } \frac{\sigma_i}{\sigma_1} > \delta_{hi} \\ \frac{1}{\delta_{hi}\sigma_1} & \text{if } \delta_{hi} \geq \frac{\sigma_i}{\sigma_1} \geq \delta_{lo} > 0 \\ 0 & \text{if } \frac{\sigma_i}{\sigma_1} < \delta_{lo}. \end{cases} \quad (7)$$

Hence, directions with small singular values which represent high gains from τ_c to T in the naive pseudo-inversion approach are ignored. Since these directions do not represent any significant mean environmental disturbance, high-frequency disturbance components of τ_c are efficiently ignored. Although τ_c is derived from a Kalman Filter approach where disturbance models are considered, not all of the high-frequency disturbances will be removed from the command vector τ_c when high overall control bandwidth is required.

When the thrust T has been determined, thruster models can be used to determine the corresponding rpm or pitch for the fixed pitch propellers or controllable pitch propellers, respectively. The thruster characteristics provided by the thruster

Table 1. Ship data.

Overall length of ship	210 m
Length between perpendiculars	200 m
Breadth	36 m
Depth	20 m
Draft to design waterline	20 m
Dead weight	90000 tons

Table 2. Simulation data.

Wind velocity	14 m/s
Wind direction	200 degrees
Significant wave height	5.9 m
Current velocity	0.5 m/s
Current direction	195 degrees
Azimuth filter time constant	200 s
Controller parameter: δ_{hi}	0.5
Controller parameter: δ_{lo}	0.1

and propeller manufacturers can be further updated by identification as in (Fossen et al. 1996).

Remark 1. In robotics, the problem of singularities has been solved with damped least-squares solutions, where the singular values are adjusted to increase the smallest singular value and hence avoid high gains in the inverse kinematics, see (Chiaverini et al. 1994) for a review. Here, instead of adjusting the singular values, the components in the reference τ_c corresponding to directions with small singular values are completely ignored yielding also an efficient filtering of the high frequency disturbances without reducing the performance.

5. SIMULATIONS

The proposed scheme for thrust allocation with the azimuth angles given in (2) and the thrusts given in (6) was tested in a Matlab simulator developed at ABB Industri AS, Norway, for the dynamic positioning of ships. A ship model was used with three azimuth thrusters, as for the ship in Fig. 1. There are three azimuth thrusters that can rotate in all directions. The thrusters are bi-directional controllable pitch (CP) thrusters. CP thrusters apply forces by turning the propeller blades. Realistic models for current-, wind-, and wave-induced disturbance forces were included. Data for the ship are shown in Table 1.

The simulation data are shown in Table 2. The controller parameters δ_{hi} and δ_{lo} determines the modified pseudo inverse S_δ^+ according to (6–7).

In Fig. 7 the resulting azimuth angles are shown when using the proposed thrust allocation. It is seen that the angles are slowly varying.

In Fig. 8 the resulting pitch ratio values are shown, indicating the thrust from each thruster. In this case, the pitch ratio values can vary within $[-1, 1]$. Note that the applied thrust is mainly positive.

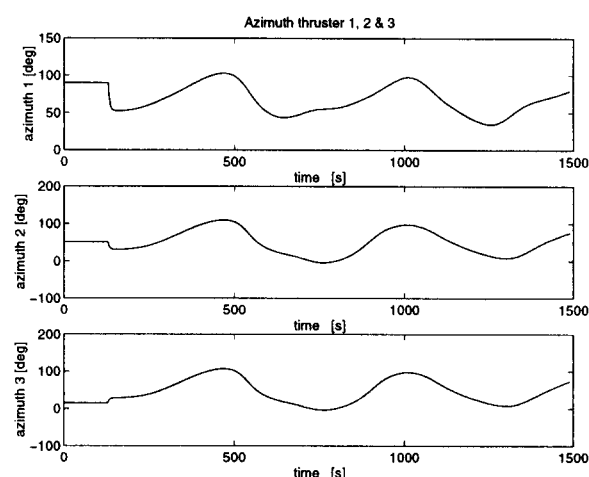


Fig. 7. Azimuth angles when using the singular-value-based thrust allocation.

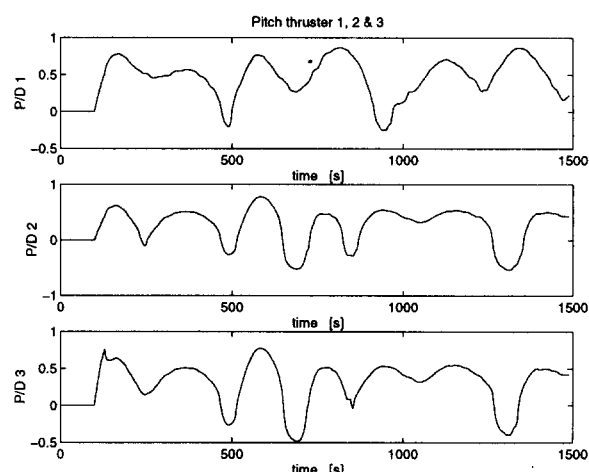


Fig. 8. Pitch ratio values when using the singular-value-based thrust allocation.

Also some negative thrust is applied instead of turning the azimuths by 180° .

For comparison, the same simulation was run in the case of fixed thruster directions and simple pseudo inversion. The thruster directions were fixed at

$$[\alpha_1, \alpha_2, \alpha_3]^T = [90^\circ, 120^\circ, -120^\circ]^T$$

which is a configuration which spans the thrust space well, i.e. the configuration is far from any singular configuration. The resulting pitch values are shown in Fig. 9.

It is seen that fixed thruster directions lead to saturations in the pitch in this case, whereas the singular-value-based thrust allocation reduces the pitch required and avoids saturation.

6. FULL-SCALE SEA TRIALS

The proposed thrust-allocation scheme has been successfully implemented in ABB positioning sys-

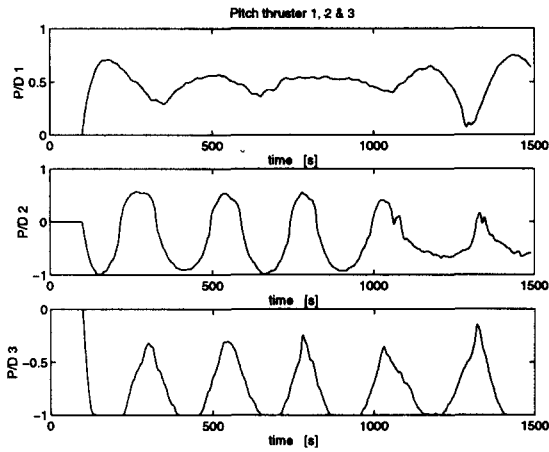


Fig. 9. Pitch ratios when using fixed thruster directions and pseudo-inversion.

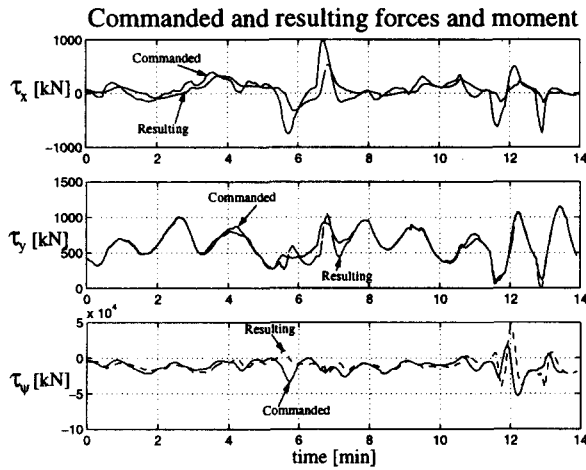


Fig. 10. Commanded and resulting forces in surge and sway, and yaw moment.

tems for dynamic positioning, thruster-assisted mooring, and auto sail.

Full-scale sea trials were performed on a floating production vessel with data as given in Table 1. The thruster configuration of the vessel is as shown in Fig. 1. The three azimuth thrusters were bi-directional CP thrusters. Fig. 10 shows the commanded forces and moment from the control law, together with the resulting forces and moment from the thrust allocation. This figure shows that these forces and moments are quite similar, although not identical since the smallest singular value is neglected in the modified pseudo-inversion (6). The reason for the deviation is the trade-off between the constraint items (1) and (2).

The corresponding pitch signals are shown in Fig. 11 as a percentage of the maximum pitch values. It is observed that the pitch values are relatively small and mainly positive, which is more efficient than negative pitch. The sign of the pitch, and hence the thrust, is due to the filtering scheme for the azimuth angles. This figure shows that the

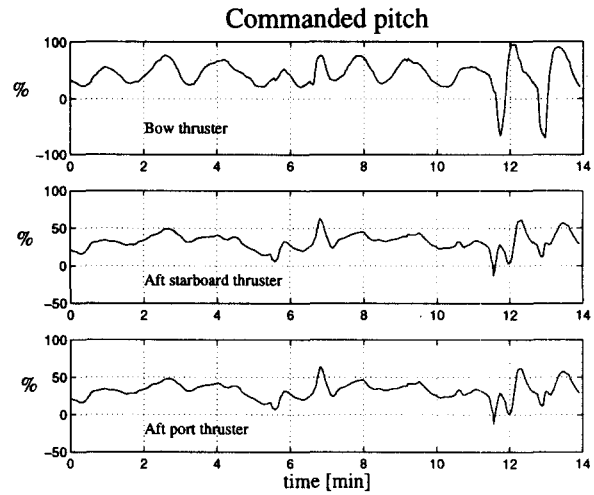


Fig. 11. Commanded pitch with the proposed thrust allocation.

pitch can become negative for some time, also, which is more efficient than turning the azimuths by 180° as soon as the commanded thrust goes negative.

In Fig. 12 the corresponding azimuth angles are shown as a function of time. The bandwidth of these signals can be specified by a control parameter in the azimuth angle-filtration scheme. This figure also shows some hold phases of some of the azimuths. This "freezing" of the azimuths is due to the introduction of forbidden sectors of the azimuth angles. Such sectors can be defined for each azimuth thruster, to avoid the jet beam from one azimuth thruster reducing the performance of a neighboring thruster, or disturbing underwater equipment installed on the ship's hull. In the experiments, the forbidden sector for the aft starboard thruster was set to $90^\circ \pm 5^\circ$. In addition to the feature of possible forbidden sectors, another feature has been implemented; the rotation of the azimuths is stopped if the desired azimuth angle is within a certain specified deviation of the actual azimuth angle.

The resulting singular values of the normalized matrix $A(\alpha)$, i.e. the last row corresponding to the moment has been divided by the length of the vessel, are plotted in Fig. 13. A singular value close to zero shows that the azimuths have been oriented very close to singular configurations. These configurations give the lowest thrust with respect to the low-frequency part of τ_c . However, due to the small singular value, the thrust T becomes very sensitive to the high-frequency part, corresponding to disturbances, of τ_c if a naive inversion of $A(\alpha)$ is used to determine T . With the thrust-allocation approach proposed and implemented here, the components of τ_c corresponding to the small singular values are ignored, and low-thrust T is obtained without large deviations of the re-

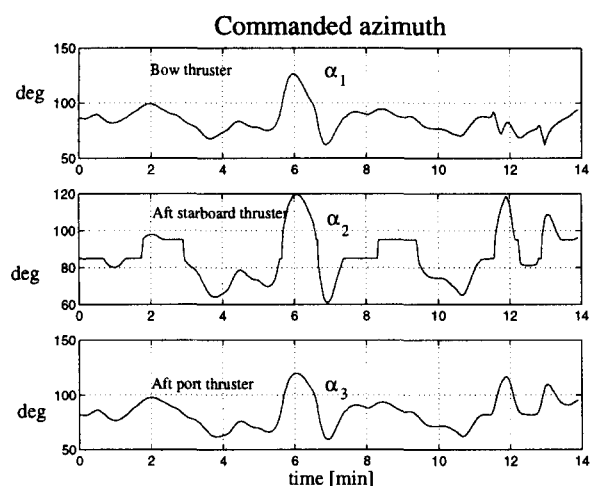


Fig. 12. Resulting azimuth angles with the proposed thrust allocation.

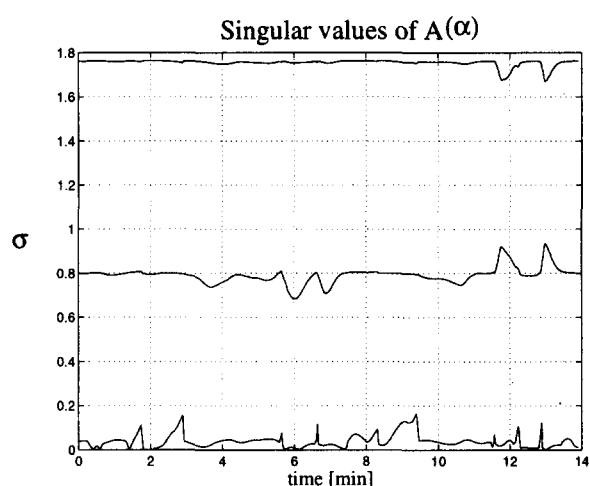


Fig. 13. Plot of resulting singular values of $A(\alpha(t))$.

sulting thrusts and moment from commanded τ_c , as seen from Fig. 10.

From Fig. 14 it is seen that the resulting vessel position remains within ± 3 m of the desired position. The environmental data were: wind velocity was 14 m/s, the current was 1 m/s, and the significant wave height was 1.5 m.

Fig. 15 shows that the resulting heading is kept within $\pm 0.5^\circ$ of the reference of 201° .

The result with the proposed thrust allocation was compared with a case with fixed azimuths, which is one solution to avoid the problems with singularities. The azimuths were fixed in the configuration $\alpha = [90^\circ, -120^\circ, 120^\circ]^T$, as in the simulation, which is a configuration where one has good maneuverability in all directions: surge, sway, and yaw. The pitch values were found from the thrust models based on $T = A^{-1}(\alpha) \tau_c$. The pitch values are plotted in Fig. 16 as dashed lines for constant azimuths, and as solid lines for automatic control of azimuth angles as proposed here.

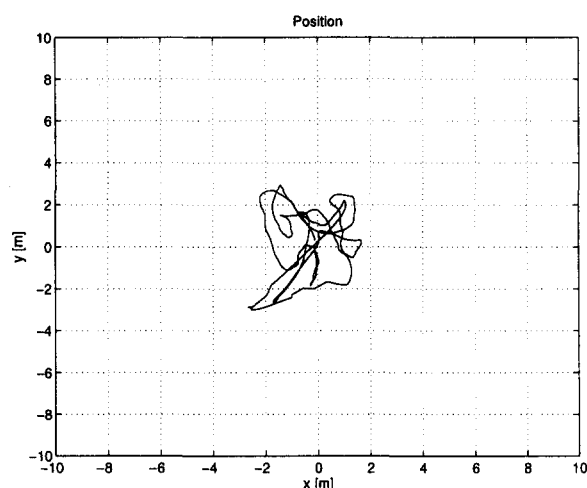


Fig. 14. Resulting position of the vessel with the proposed thrust allocation during dynamic positioning.

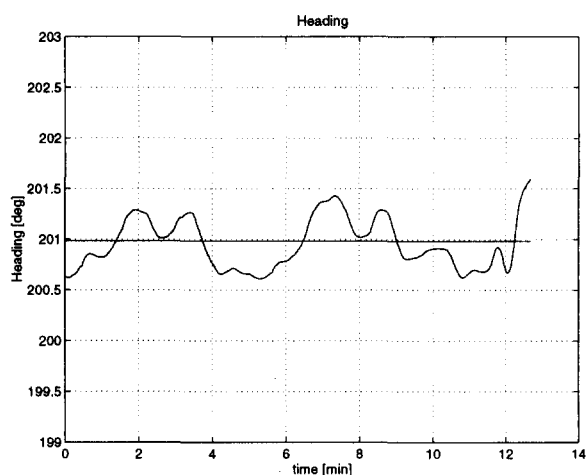


Fig. 15. Resulting heading of the vessel with the proposed thrust allocation during dynamic positioning.

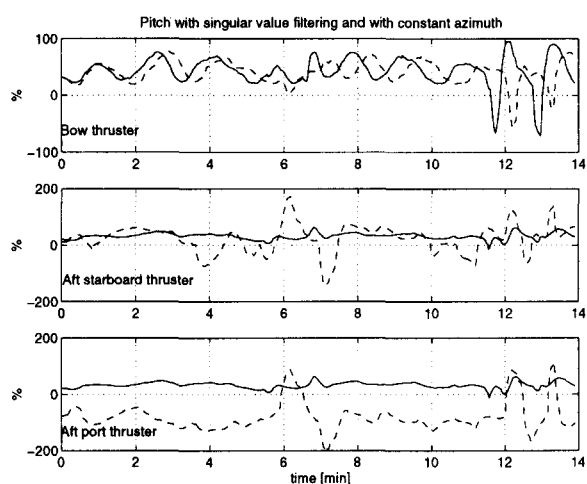


Fig. 16. Comparison of pitch values for constant azimuth angles and automatic controlled azimuth angles as proposed here. The dashed line shows the case with constant azimuth angles.

Table 3. Relative fuel consumption (RFC) with the proposed thrust allocation, compared to the case with fixed azimuth angles in $\alpha = [90^\circ, -\psi, \psi]^T$.

ψ	100°	110°	120°	130°	140°	150°
RFC	51%	64%	69%	70%	67%	60%

The power consumption has been modelled as function of the pitch values using data about the actual thrusters. By using these models the energy consumption of the cases with fixed and automatic azimuths have been compared. During the 14 minutes of logging, the energy consumption with the control of the azimuths proposed here was only 69% of the energy consumption resulting from fixed azimuth angles in $\alpha = [90^\circ, -120^\circ, 120^\circ]^T$. Similar calculations were done for various cases of fixed azimuth angles with configurations $\alpha = [90^\circ, -\psi, \psi]^T$. The relative energy/fuel consumption with the proposed thrust allocation is shown in Table 3 for various angles ψ , indicating a very efficient thrust-allocation scheme.

7. CONCLUSIONS

The problem of singular configurations of thruster devices have been pointed out. A thrust allocation scheme including active azimuth control has been proposed, and has been implemented in the ABB positioning systems. Due to a filtering scheme, the azimuth thrusters point in directions that reduce the thrust and power needed to counteract the mean environmental disturbances. To ensure the avoidance of high thrust close to singular configurations, the singular value decomposition is performed and the smallest singular values are analyzed, resulting in cancellations of (high-frequency) components of the commanded forces and moment. The thrust-allocation algorithm presented here does not involve any iterations, and is easy to reconfigure for various thruster configurations. Moreover, the thrust allocation is energy-efficient. Full-scale sea trials showed that the energy consumption is reduced by more than 30% without reducing the performance.

Other features of the implemented thrust-allocation scheme, such as

- forbidden sectors for azimuth directions
- freezing the azimuth motion to reduce wear and tear
- thrust reduction in order not to exceed the power limits of thruster motors and power buses

have been successfully demonstrated with high performance and flexibility in real operation.

8. ACKNOWLEDGMENT

The author would like to thank the Marine Division at ABB Industri AS, Norway, for co-operating in the development, and for allowing the presentation of the full-scale results.

9. REFERENCES

- Balchen, J. G., N. A. Jensen, E. Mathisen and S. Sælid (1980). Dynamic positioning systems based on kalman filtering and optimal control. *Modeling, Identification and Control* 1(3), 135–163.
- Chiaverini, S., B. Siciliano and O. Egeland (1994). Review of the damped least-squares inverse kinematics with experiments on an industrial robot manipulator. *IEEE Transactions on Control Systems Technology* 2(2), 123–134.
- Fossen, T. I. (1994). *Guidance and control of Ocean Vehicles*. Wiley.
- Fossen, T. I., S. I. Sagatun and A. J. Sørensen (1996). Identification of dynamically positioned ships. *Control Eng. Practice* 4(3), 369–376.
- Jensen, N. A. (1980). Estimation and Control in Dynamic Positioning of Vessels. PhD thesis. The Norwegian Institute of Technology. ITK-report 80-90-W.
- Lindfors, I. (1993). Thrust allocation method for the dynamic positioning system. In: *10th International Ship Control Systems Symposium (SCSS'93)*. Ottawa, Canada. pp. 3.93–3.106.
- Sørdalen, O. J. (1996). Thruster allocation: Singularities and filtering. In: *13th World Congress of IFAC*. Vol. Q. San Francisco, California. pp. 369–374.
- Sørensen, A. J., S. I. Sagatun and T. I. Fossen (1996). Design of a dynamic positioning system using model-based control. *Control Eng. Practice* 4(3), 359–368.
- Strang, G. (1980). *Linear Algebra and Its Applications*. Academic Press.